

# Preliminary Study of $^{11}\text{C}$ -Choline PET/CT for T Staging of Locally Advanced Nasopharyngeal Carcinoma: Comparison with $^{18}\text{F}$ -FDG PET/CT

Hu-bing Wu<sup>1</sup>, Quan-shi Wang<sup>1</sup>, Ming-fang Wang<sup>1</sup>, Xiaokang Zhen<sup>2</sup>, Wen-lan Zhou<sup>1</sup>, and Hong-sheng Li<sup>1</sup>

<sup>1</sup>NanFang PET Center, Nanfang Hospital, Southern Medical University, Guangzhou, China; and <sup>2</sup>Department of Radiotherapy, Nanfang Hospital, Southern Medical University, Guangzhou, China

Evaluation of nasopharyngeal carcinoma (NPC) using  $^{18}\text{F}$ -FDG PET/CT is limited by the intense physiologic uptake of  $^{18}\text{F}$ -FDG in the brain. We attempted to improve detection of intracranial tumor invasion (including better delineation of invasion near the skull base) in locally advanced NPC using  $^{11}\text{C}$ -choline PET/CT. **Methods:** Fifteen patients with newly diagnosed or recurrent locally advanced NPC were enrolled in the study.  $^{18}\text{F}$ -FDG and  $^{11}\text{C}$ -choline PET/CT was performed on all patients. PET/CT images obtained using the 2 tracers were compared using both maximum standardized uptake value (SUVmax) and tumor-to-brain (T/B) ratios. All patients were followed up for more than 1 y. **Results:** The sensitivity of  $^{18}\text{F}$ -FDG PET/CT in detecting locally advanced NPC was 86.6%, compared with a 100% sensitivity for  $^{11}\text{C}$ -choline PET/CT ( $t = 2.143$ ,  $P = 0.483$ ). The SUVmax of lesions detected was higher using  $^{18}\text{F}$ -FDG than using  $^{11}\text{C}$ -choline ( $12.81 \pm 5.00$  vs.  $6.84 \pm 2.76$ ,  $t = 6.416$ ,  $P < 0.001$ ), but the T/B ratio was much higher for  $^{11}\text{C}$ -choline than for  $^{18}\text{F}$ -FDG ( $18.62 \pm 7.95$  vs.  $1.38 \pm 0.59$ ,  $t = 8.801$ ,  $P < 0.001$ ). Compared with  $^{18}\text{F}$ -FDG PET/CT,  $^{11}\text{C}$ -choline PET/CT improved the delineation of intracranial invasion in 6 of 12 patients ( $\chi^2 = 8.00$ ,  $P = 0.014$ ), skull base invasion in 4 of 14 patients, and orbital invasion in 3 of 3 patients. **Conclusion:**  $^{11}\text{C}$ -choline can improve the quality of PET/CT in the T staging of NPC.

**Key Words:** nasopharyngeal carcinoma, T staging, PET/CT,  $^{11}\text{C}$ -choline;  $^{18}\text{F}$ -FDG

**J Nucl Med 2011; 52:341–346**

DOI: 10.2967/jnumed.110.081190

**N**asopharyngeal carcinoma (NPC) is a common malignancy in southern China, with intracranial as well as skull base invasion frequently seen in patients with locally advanced disease. The determination of the gross tumor volume and delineation of the extent of tumor invasion are critical for radiation treatment planning (1–3).

$^{18}\text{F}$ -FDG PET/CT has been shown to be more accurate than MRI for the detection of cervical nodal metastasis of NPC and to be more accurate than conventional work-up (chest radiography, liver ultrasound, skeletal scintigraphy, and CT of the thorax and abdomen) for detection of distant metastases (1,3–8). However,  $^{18}\text{F}$ -FDG PET/CT lacks sensitivity for T staging, especially in the delineation of skull base and intracranial invasion, because of the intense physiologic uptake of  $^{18}\text{F}$ -FDG in the brain (8,9).  $^{11}\text{C}$ -choline has been introduced as a complementary tumor imaging agent for gliomas and other brain tumors because its uptake in normal brain is minimal (10–12). In the present study, we investigated whether  $^{11}\text{C}$ -choline can improve the quality of PET/CT in T staging of NPC.

## MATERIALS AND METHODS

### Patients

The study was approved by our hospital's Institutional Review Board, and all subjects gave written informed consent before their participation in the study.

From December 2007 through May 2009, 15 patients (including 10 men and 5 women, with a mean age of 49 y [range, 36–76 y]) were enrolled in the study. Ten of the patients were newly diagnosed, and 5 had recurrent locally advanced NPC. The 15 cases of NPC, diagnosed by histopathology, included 14 cases of nonkeratinizing undifferentiated carcinoma and 1 case of well-differentiated squamous carcinoma. Intracranial and skull base invasion was diagnosed using contrast-enhanced MRI or CT combined with other clinical findings, such as the cranial nerve sign. The clinical data are listed in Table 1. All patients were treated with radical radiotherapy and chemotherapy and were followed up for a mean of 19 mo (range, 14–26 mo).

### $^{18}\text{F}$ -FDG and $^{11}\text{C}$ -Choline PET/CT Examination

All examinations were performed using a Discovery LS PET/CT scanner (GE Healthcare). The patients were instructed to fast for at least 6 h, and blood glucose was monitored immediately before the study to ensure a normal blood glucose level ( $<7$  mmol/L). Approximately 60 min after the intravenous injection of 315–511 MBq (8.49–13.81 mCi, 150  $\mu\text{Ci}/\text{kg}$ ) of  $^{18}\text{F}$ -FDG, whole-body PET/CT was performed, according to published guidelines for tumor imaging with  $^{18}\text{F}$ -FDG PET/CT (13). The patients also underwent regional PET/CT of the head and neck at approximately 10 min after the intravenous injection of 370–

Received Jul. 12, 2010; revision accepted Dec. 1, 2010.

For correspondence or reprints contact: Quan-shi Wang, NanFang PET Center, Nanfang Hospital, Southern Medical University, 1838 Guangzhou Ave. N., Guangzhou, Guangdong Province, 510515, China.

E-mail: wqsiph@163.net

COPYRIGHT © 2011 by the Society of Nuclear Medicine, Inc.

**TABLE 1**  
Clinical Data on NPC Patients

Patient no.	Sex	Age (y)	Diagnosis	Pathology	Cranial nerve sign	Lesion invasion				Confirmation
						Nasopharynx	Skull base	Brain	Orbit	
1	M	41	ND	NKUC	+	+	+	-	-	MRI (CE)
2	M	58	ND	NKUC	+	+	+	+	-	MRI (CE)
3	F	45	Recurrence	NKUC	+	-	-	+	-	MRI (CE)
4	M	47	ND	NKUC	+	+	+	+	-	MRI (CE)
5	F	42	ND	NKUC	+	+	+	+	-	CT (CE)
6	M	68	Recurrence	NKUC	+	+	+	-	+	MRI (CE)
7	F	76	ND	NKUC	+	+	+	+	-	CT (CE)
8	F	49	ND	NKUC	+	+	+	+	+	MRI (CE)
9	M	36	ND	NKUC	+	+	+	+	-	MRI (CE)
10	M	41	ND	NKUC	-	+	+	-	-	CT (CE)
11	M	41	ND	NKUC	+	+	+	+	-	MRI (CE)
12	F	55	Recurrence	NKUC	+	-	+	+	-	MRI (CE)
13	M	37	ND	NKUC	+	+	+	+	+	CT (CE)
14	M	55	Recurrence	NKUC	+	+	+	+	-	MRI (CE)
15	F	45	Recurrence	WDSC	+	-	+	+	-	MRI (CE)

NKUC = nonkeratinizing undifferentiated carcinoma; + = positive; - = negative; CE = contrast enhanced; WDSC = well differentiated squamous carcinoma.

740 MBq (10.0–20.0 mCi) of  $^{11}\text{C}$ -choline during fasting.  $^{11}\text{C}$ -choline was produced by the method of Wilson et al. (14), and the radiochemical purity exceeded 99%.

Image acquisition using whole-body  $^{18}\text{F}$ -FDG PET/CT included 6–8 bed positions for each unenhanced CT and PET scan, covering the entire range from the vertex of the skull to the mid thigh using head fixation. If head movement was noted, then imaging was performed at an additional bed position covering the lesion. Image acquisition using  $^{11}\text{C}$ -choline PET/CT, performed on a different day, included 2 bed positions covering the head and neck. Each CT scan was performed with a scout view using 20 mA and 80 kVp, followed by a spiral CT scan with a 0.8-s rotation time, 80 mA, 140 kVp, a 5-mm section thickness, and a 4.25-mm interval in high-speed mode. After CT was completed, the scanner was returned to the landmark position and the PET scan was then acquired in the 2-dimensional acquisition mode at 4 min per 14.25-cm bed position. Among the 15 patients enrolled, a 3-dimensional acquisition brain scan was performed on 2 patients who were suspected to have intracranial recurrence but showed no abnormality on the 2-dimensional-mode  $^{18}\text{F}$ -FDG whole-body scan.  $^{11}\text{C}$ -choline PET/CT was performed using the same acquisition method as that used for the  $^{18}\text{F}$ -FDG PET/CT scans.

The PET images were reconstructed using a standard iterative algorithm (ordered-subset expectation maximization), with the CT data used for attenuation correction. The 2 PET/CT scans were performed on 2 different days, and all scans were completed within 1 wk. No treatment was performed during this period.

### Image Analysis

The acquired PET and CT images were sent to the Xeleris workstation (GE Healthcare) for registration and fusion. The images from both  $^{18}\text{F}$ -FDG and  $^{11}\text{C}$ -choline PET/CT scans were reviewed separately on different days by 2 experienced nuclear medicine physicians, who were unaware of the results of contrast-enhanced MRI/CT. Each reviewer independently assessed each  $^{18}\text{F}$ -FDG and  $^{11}\text{C}$ -choline image. After visually examining all images on the

workstation, the reviewers reached a final diagnosis based mainly on fusion images of PET and CT. Any initial difference of opinion was resolved by consensus. A lesion showing  $^{11}\text{C}$ -choline or  $^{18}\text{F}$ -FDG uptake that exceeded that of the surrounding normal tissue was considered positive. The border of each lesion was visually evaluated by comparing the radioactivity at the margin of the lesion with that of the surrounding normal tissue. If the radioactivity at the margin of the lesion was higher than that of the surrounding normal tissue, then the borders and the extent of invasion were determined. The syn-modality CT was used to determine morphologic location and degree of invasion. After separately interpreting each modality, 2 experienced nuclear medicine physicians comparatively analyzed the fused images of the 2 modalities frame by frame. The scope and border of each lesion were compared, and any discrepancy between the 2 modalities was recorded. The physiologic uptake of  $^{18}\text{F}$ -FDG in the ocular muscles was carefully analyzed to avoid a potential false-positive result.

For measurement of the maximum standardized uptake values (SUVmax), the region of interest was drawn along the margin of the lesion on the transverse PET image. For determination of uptake in normal brain tissue, a circular 2-cm region of interest was placed on the normal contralateral cerebellum. The tumor-to-brain (T/B) ratio was calculated by dividing the SUVmax of each lesion by that of the contralateral normal cerebellum.  $^{11}\text{C}$ -choline PET/CT images were selected for size measurements because they showed a clear tumor border. The longest major axis measured in any section that contained tumor was defined as the maximum diameter of the tumor.

### Statistical Analysis

The SUVmax and T/B ratio were expressed as the mean  $\pm$  the SD. Statistical Package for the Social Sciences, version 13.0 (SPSS Inc.), was used for statistical analysis, and the paired *t* test was used to compare the 2 paired samples. The rates were compared using the crosstabs  $\chi^2$  test. A *P* value of less than 0.05 was considered statistically significant.

**TABLE 2**  
Visual Evaluation of Tumor Invasion Using the 2 Modalities

Diagnosis	n	Detection		Visual evaluation		
		<sup>11</sup> C-choline	<sup>18</sup> F-FDG	<sup>11</sup> C-choline = <sup>18</sup> F-FDG	<sup>11</sup> C-choline > <sup>18</sup> F-FDG	<sup>18</sup> F-FDG > <sup>11</sup> C-choline
Nasopharynx	12	12	12	12	0	0
Skull base	14	14	12	9	4	1
Brain	12	12	10	6	6	0
Orbit	3	3	0	0	3	0

Equals sign indicates similar clear border or similar large extent. Greater-than sign indicates clearer border or larger extent or when <sup>11</sup>C-choline PET/CT was positive and <sup>18</sup>F-FDG PET/CT was negative.

## RESULTS

### Semiquantitative Analysis of the 2 PET Studies

Ten of the 15 patients had newly diagnosed NPC, and 5 patients had recurrent NPC. <sup>18</sup>F-FDG PET/CT was positive for tumor in all 10 newly diagnosed NPC patients and was positive in 3 of 5 cases of recurrent tumor. In 2 patients with insidious skull base involvement and intracranial recurrence, <sup>18</sup>F-FDG PET/CT was negative. However, <sup>11</sup>C-choline was positive in all 15 NPC patients. The sensitivity for the positive detection of tumor was 86.6% using <sup>18</sup>F-FDG PET/CT, compared with 100% using <sup>11</sup>C-choline PET/CT ( $t = 2.143, P = 0.483$ ).

Overall uptake of radiotracer in lesions was higher for <sup>18</sup>F-FDG than for <sup>11</sup>C-choline (SUVmax,  $12.81 \pm 5.00$  vs.  $6.84 \pm 2.76, t = 6.416, P < 0.000$ ), but <sup>11</sup>C-choline had a much higher T/B ratio than did <sup>18</sup>F-FDG ( $18.62 \pm 7.95$  vs.  $1.38 \pm 0.59, t = 8.801, P < 0.001$ ). This result is likely due to the

lower uptake of <sup>11</sup>C-choline than of <sup>18</sup>F-FDG in normal brain ( $0.38 \pm 0.09$  vs.  $10.01 \pm 1.90, t = 19.68, P < 0.001$ ). A significant correlation was found between the 2 tracers with regard to lesion uptake ( $r = 0.712, P = 0.003$ ). In addition, there was also a significant correlation between lesion size and tracer uptake for both radiotracers (<sup>18</sup>F-FDG:  $r = 0.790, P < 0.001$ ; <sup>11</sup>C-choline:  $r = 0.759, P = 0.001$ ).

### Visual Evaluation of Tumor Delineation

**Nasopharyngeal Invasion.** Twelve patients had lesions in the nasopharynx. Intense uptake was clearly seen in all lesions for both <sup>18</sup>F-FDG and <sup>11</sup>C-choline, with each having a 100% positive detection rate. The borders and extent of invasion were clearly delineated by both modalities. The shape and size of the lesions were similar for both tracers (Table 2; Fig. 1).

**Skull Base Invasion.** Fourteen patients had skull base invasion. <sup>11</sup>C-choline PET/CT and <sup>18</sup>F-FDG PET/CT had a

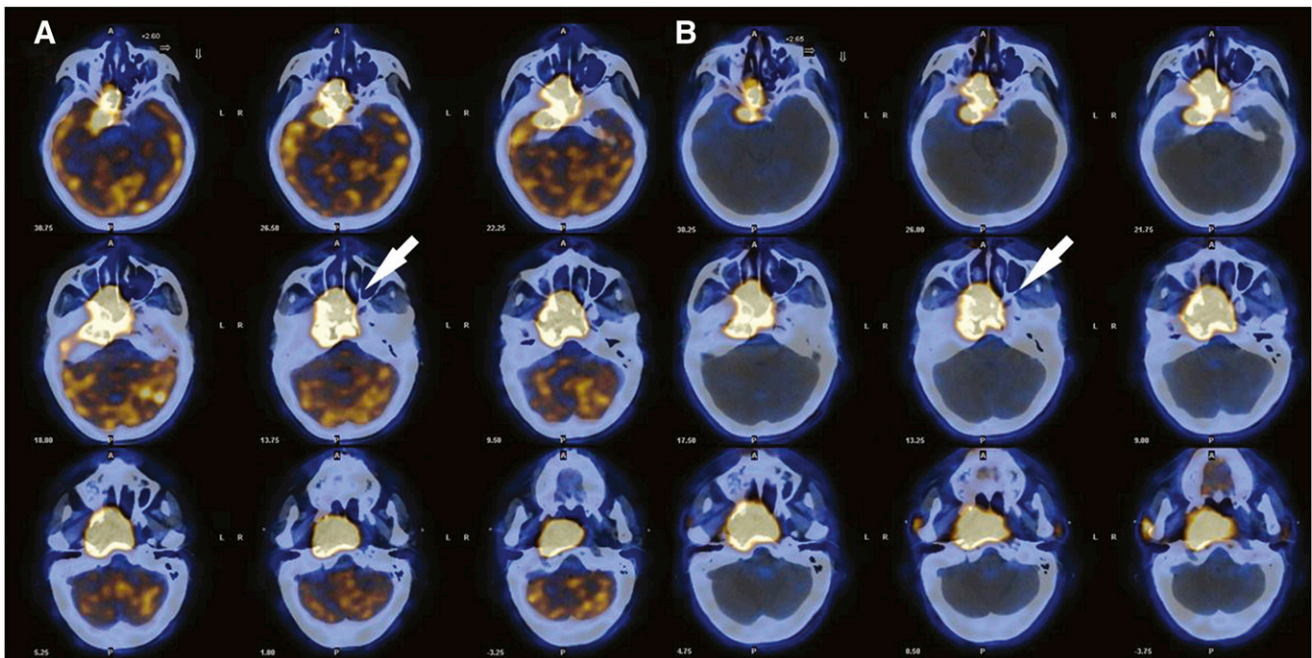


**FIGURE 1.** A 42-year-old woman with nonkeratinizing undifferentiated carcinoma of right nasopharynx. <sup>18</sup>F-FDG PET/CT (A) and <sup>11</sup>C-choline PET/CT (B) demonstrate intense uptake of both radiotracers in primary tumor (arrow), with clear and similar delineation of intracranial and skull base extension. SUVmax and T/B ratio of <sup>18</sup>F-FDG were 17.82 and 2.48, respectively, and SUVmax and T/B ratio of <sup>11</sup>C-choline were 6.17 and 23.7, respectively.

100% (14/14) and 85.7% (12/14) positive rate of detection, respectively ( $\chi^2 = 2.154$ ,  $P = 0.481$ ).  $^{11}\text{C}$ -choline and  $^{18}\text{F}$ -FDG PET/CT showed a similar tumor extent and border delineation in 9 patients. However, visual findings were discordant in 5 patients. In 4 of 14 patients (28.5%),  $^{11}\text{C}$ -choline PET/CT showed a larger extent of tumor invasion and a clearer border with respect to skull base invasion than did  $^{18}\text{F}$ -FDG PET/CT (Figs. 2E and 2F). The tumor invasion primarily involved the sphenoidal sinus, foramen lacerum, clivus basilaris, and carotid foramen. In contrast,  $^{18}\text{F}$ -FDG PET/CT was superior to  $^{11}\text{C}$ -choline PET/CT in 1 patient (Table 2).

**Intracranial Invasion.** Twelve patients were known to have intracranial invasion. Intracranial invasion was detected in 100% of patients using  $^{11}\text{C}$ -choline and in 83.3% of patients using  $^{18}\text{F}$ -FDG PET/CT ( $\chi^2 = 1.104$ ,  $P = 1.000$ ). In 2 patients with insidious intracranial recurrent tumor,  $^{18}\text{F}$ -FDG PET/CT was negative. The extent of intracranial invasion was clearly delineated by  $^{11}\text{C}$ -choline PET/CT (Figs. 2 and 3) in all 12 patients and by  $^{18}\text{F}$ -FDG PET/CT in only 6 patients. Thus,  $^{11}\text{C}$ -choline PET/CT

improved the visual determination of intracranial invasion in 50% (6/12) of patients ( $\chi^2 = 8.00$ ,  $P = 0.014$ ).

**Orbital Invasion.** Three patients were known to have orbital invasion. Orbital invasion was clearly visualized in all 3 patients using  $^{11}\text{C}$ -choline PET/CT (Fig. 2D), but  $^{18}\text{F}$ -FDG PET/CT was either negative or indeterminate because of physiologic uptake of  $^{18}\text{F}$ -FDG in the ocular muscles (Fig. 2C).

## DISCUSSION

Several articles have shown that  $^{18}\text{F}$ -FDG PET/CT plays an important role in the diagnosis and staging of NPC.  $^{18}\text{F}$ -FDG PET/CT was reported to be superior to MRI and conventional work-up (chest radiography, liver ultrasound, skeletal scintigraphy, and CT of the thorax and abdomen) for the detection of cervical lymph node metastasis and distant metastasis (4–8).  $^{18}\text{F}$ -FDG PET/CT was also reported to have a positive impact on radiotherapy planning and patient management (15–17). But for the T staging of locally advanced NPC, the studies of Ng et al. and King et al. have indicated that  $^{18}\text{F}$ -FDG PET/CT may underestimate the presence or extent of tumor invasion in the para-

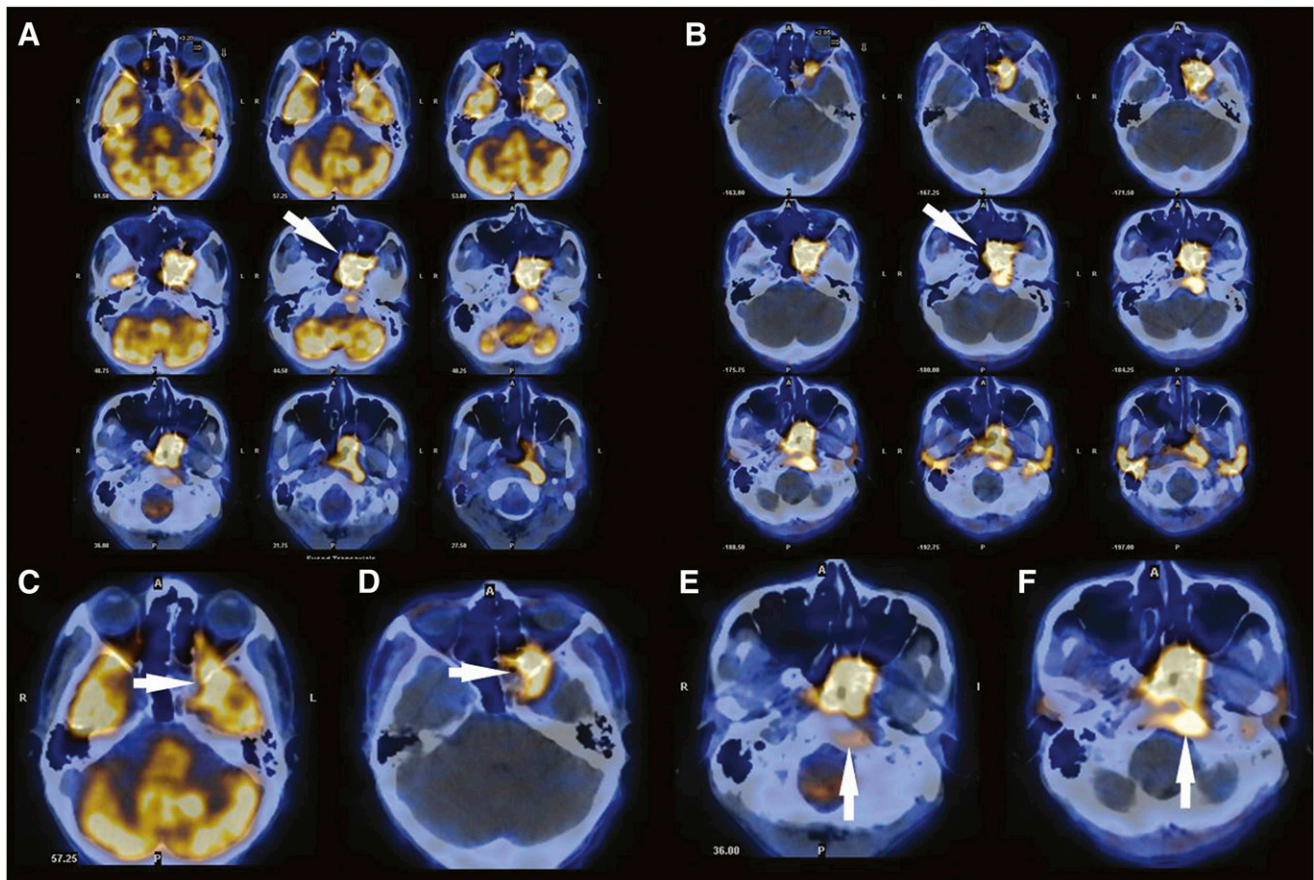


**FIGURE 2.** A 37-y-old man with nonkeratinizing undifferentiated carcinoma of left nasopharynx.  $^{18}\text{F}$ -FDG (A) and  $^{11}\text{C}$ -choline PET/CT (B) both demonstrate intense tracer uptake at primary site of NPC (arrow). SUVmax and T/B ratio of  $^{18}\text{F}$ -FDG in lesion were 11.21 and 1.05, respectively, and SUVmax and T/B ratio of  $^{11}\text{C}$ -choline were 7.86 and 25.3, respectively. Both modalities demonstrate invasion of nasopharynx, parapharyngeal region, skull base, and left temporal lobe.  $^{11}\text{C}$ -choline PET/CT (D) shows clearer border of invasion of left orbit and left temporal lobe (arrow) than does  $^{18}\text{F}$ -FDG PET/CT (C). Extent of clivus basilaris invasion (arrow) is also clearer and larger with  $^{11}\text{C}$ -choline PET/CT (F) than with  $^{18}\text{F}$ -FDG PET/CT (E).

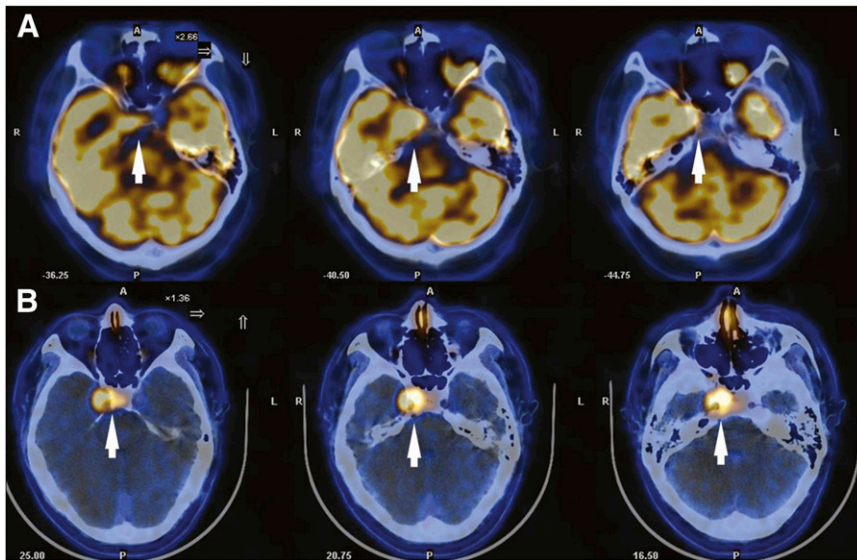


**FIGURE 3.** A 36-y-old man with recurrent NPC of right nasopharynx.  $^{18}\text{F}$ -FDG PET/CT (A) shows increased uptake of  $^{18}\text{F}$ -FDG in skull base and adjacent right temporal lobe (arrow, SUVmax = 13.66), with unclear border (T/B ratio = 1.04). Uptake of  $^{11}\text{C}$ -choline in skull base and left temporal lobe is intense (arrow, SUVmax = 6.00). Clearer border of intracranial invasion is seen with  $^{11}\text{C}$ -choline PET/CT (B) (T/B ratio = 10.71) than with  $^{18}\text{F}$ -FDG PET/CT.

pharyngeal space, skull base, intracranial area, sphenoid sinus, and retropharyngeal nodes, when compared with MRI (8,9).

Our results confirmed that  $^{18}\text{F}$ -FDG PET/CT is limited with regard to T staging for locally advanced NPC.  $^{18}\text{F}$ -FDG PET/CT underestimated invasion of the skull base, intracranial compartment, and orbit in 4 of 14, 6 of 12, and 3 of 3 patients, respectively, when compared with  $^{11}\text{C}$ -choline PET/CT. This discrepancy is likely due to the higher physiologic uptake of  $^{18}\text{F}$ -FDG in normal brain, which makes intracalvarial lesions or lesions near the skull base difficult to detect on  $^{18}\text{F}$ -FDG PET/CT. In addition, high physiologic uptake of  $^{18}\text{F}$ -FDG in the ocular muscles may also obscure orbital invasion.

Radiolabeled choline is a novel PET agent for tumor imaging. Radioactive choline can rapidly incorporate into tumor cells and then through phosphorylation become phosphorylcholine and finally integrate into a phospholipid—that is, phosphatidylcholine (18,19). High uptake of radioactive choline has been confirmed in many types of tumors, such as prostate carcinoma, brain tumors, hepatocellular carcinoma, and bone and soft-tissue sarcoma (20–29). To our knowledge, however, no one has evaluated the use of  $^{11}\text{C}$ -choline PET/CT for the diagnosis of NPC. In addition, uptake of  $^{11}\text{C}$ -choline in the normal brain was reported to be quite low, suggesting that  $^{11}\text{C}$ -choline PET/CT may be helpful for T staging of NPC, especially for the detection and delineation of intracranial invasion.

The present study demonstrated avid uptake of  $^{11}\text{C}$ -choline by NPC. The SUVmax of  $^{11}\text{C}$ -choline also correlated positively with NPC lesion size ( $P = 0.001$ ). With a low level of background radioactivity in normal brain tissue,  $^{11}\text{C}$ -choline PET/CT had a much higher T/B ratio than did  $^{18}\text{F}$ -FDG PET/CT. As a result,  $^{11}\text{C}$ -choline PET/CT improved the detection of insidious intracranial recurrence in 2 patients and the visual delineation of skull base, intra-

cranial, and orbital invasion in 4 of 14, 6 of 12, and 3 of 3 patients, respectively. This finding suggests that  $^{11}\text{C}$ -choline PET/CT may be superior to  $^{18}\text{F}$ -FDG PET/CT for determining gross tumor volume in patients with locally advanced NPC.

Although imaging plays an important role in NPC for both determining gross tumor volume and T staging, unfortunately, pathologic and radiologic findings cannot usually be correlated because few patients undergo surgical resection. Thus, evidence from the literature is scanty. MRI is known to be a highly sensitive technique for identifying tumor invasion and is currently the standard modality for T staging of NPC. However, MRI has problems with specificity that can lead, in some cases, to results that are positive due to edema and inflammation rather than to tumor infiltration (30). Daisne et al. reported that tumor volume in pharyngolaryngeal squamous cell carcinoma, as determined by  $^{18}\text{F}$ -FDG PET, was found to be more accurate than CT and MRI determinations, particularly when the volume was compared with the actual surgical specimen (31). If  $^{11}\text{C}$ -choline PET/CT were proven more accurate than MRI for tumor delineation, then  $^{11}\text{C}$ -choline PET/CT could play an important role in gross tumor volume determination, thus improving radiation treatment outcome. Future research should be undertaken to determine which technique is more accurate for tumor delineation and whether a complementary role exists between  $^{11}\text{C}$ -choline PET/CT and MRI. In addition, our study was limited by our relatively small and heterogeneous patient population. Future randomized, controlled studies, using a larger patient population, are needed to confirm our findings.

It has been reported that  $^{11}\text{C}$ -choline can also be taken up by the choroid plexus, the lateral ventricles, the plexus venosus caroticus internus, and the pituitary body, potentially limiting the detection of tumors such as glioma (11). In the present study, we found that this physiologic uptake

had no influence on T staging of NPC because most of the tumors we studied were remote from all these structures except for the pituitary body. But because the uptake of  $^{11}\text{C}$ -choline was lower in the pituitary body than in tumor, the influence of  $^{11}\text{C}$ -choline PET/CT on T staging of NPC in our patients was also limited.

## CONCLUSION

The present study has demonstrated that  $^{11}\text{C}$ -choline is avidly taken up by NPC. Because of its low background radioactivity in normal brain tissue,  $^{11}\text{C}$ -choline PET/CT had a higher T/B ratio than did  $^{18}\text{F}$ -FDG PET/CT, thus improving detection of intracranial, skull base, and orbital invasion. These findings suggest that  $^{11}\text{C}$ -choline PET/CT may be a useful modality for T staging of NPC in conjunction with  $^{18}\text{F}$ -FDG PET/CT.

## ACKNOWLEDGMENTS

We thank our colleagues in the Department of Radiotherapy, Nanfang Hospital, who provided the follow-up data.

## REFERENCES

1. Guigay J. Advances in nasopharyngeal carcinoma. *Curr Opin Oncol*. 2008; 20:264–269.
2. Afqir S, Ismaili N, Errihani H. Concurrent chemoradiotherapy in the management of advanced nasopharyngeal carcinoma: current status. *J Cancer Res Ther*. 2009;5:3–7.
3. O'Donnell HE, Plowman PN, Khaira MK, Alusi G. PET scanning and gamma knife radiosurgery in the early diagnosis and salvage “cure” of locally recurrent nasopharyngeal carcinoma. *Br J Radiol*. 2008;81:e26–e30.
4. Zhang GY, Hu WH, Liu LZ, et al. Comparison between PET/CT and MRI in diagnosing lymph node metastasis and N staging of nasopharyngeal carcinoma [in Chinese]. *Zhonghua Zhong Liu Za Zhi*. 2006;28:381–384.
5. Chua ML, Ong SC, Wee JT, et al. Comparison of 4 modalities for distant metastasis staging in endemic nasopharyngeal carcinoma. *Head Neck*. 2009;31:346–354.
6. Liu FY, Lin CY, Chang JT, et al.  $^{18}\text{F}$ -FDG PET can replace conventional work-up in primary M staging of nonkeratinizing nasopharyngeal carcinoma. *J Nucl Med*. 2007;48:1614–1619.
7. Chang JT, Chan SC, Yen TC, et al. Nasopharyngeal carcinoma staging by  $^{18}\text{F}$ -fluorodeoxyglucose positron emission tomography. *Int J Radiat Oncol Biol Phys*. 2005;62:501–507.
8. Ng SH, Chan SC, Yen TC, et al. Staging of untreated nasopharyngeal carcinoma with PET/CT: comparison with conventional imaging work-up. *Eur J Nucl Med Mol Imaging*. 2009;36:12–22.
9. King AD, Ma BB, Yau YY, et al. The impact of  $^{18}\text{F}$ -FDG PET/CT on assessment of nasopharyngeal carcinoma at diagnosis. *Br J Radiol*. 2008;81:291–298.
10. Hara T, Kosaka N, Shinoura N, et al. PET imaging of brain tumor with [methyl- $^{11}\text{C}$ ]choline. *J Nucl Med*. 1997;38:842–847.
11. Kato T, Shinoda J, Nakayama N, et al. Metabolic assessment of gliomas using  $^{11}\text{C}$ -methionine,  $^{18}\text{F}$ fluorodeoxyglucose, and  $^{11}\text{C}$ -choline positron-emission tomography. *AJNR*. 2008;29:1176–1182.
12. Utraiainen M, Komu M, Vuorinen V, et al. Evaluation of brain tumor metabolism with [ $^{11}\text{C}$ ]choline PET and  $^1\text{H}$ -MRS. *J Neurooncol*. 2003;62:329–338.
13. Delbeke D, Coleman RE, Guiberteau MJ, et al. Procedure guideline for tumor imaging with  $^{18}\text{F}$ -FDG PET/CT 1.0. *J Nucl Med*. 2006;47:885–895.
14. Wilson AA, Garcia G, Jin L, Houle S. Radiotracer synthesis from [ $^{11}\text{C}$ ]iodomethane: a remarkably simple captive solvent method. *Nucl Med Biol*. 2000;27: 529–532.
15. Zheng XK, Chen LH, Wang QS, et al. Influence of FDG-PET on computed tomography-based radiotherapy planning for locally recurrent nasopharyngeal carcinoma. *Int J Radiat Oncol Biol Phys*. 2007;69:1381–1388.
16. Gordin A, Golz A, Daizchman M, et al. Fluorine-18 fluorodeoxyglucose positron emission tomography/computed tomography imaging in patients with carcinoma of the nasopharynx: diagnostic accuracy and impact on clinical management. *Int J Radiat Oncol Biol Phys*. 2007;68:370–376.
17. Gardner M, Halimi P, Valinta D, et al. Use of single MRI and  $^{18}\text{F}$ -FDG PET-CT scans in both diagnosis and radiotherapy treatment planning in patients with head and neck cancer: advantage on target volume and critical organ delineation. *Head Neck*. 2009;31:461–467.
18. Slack BE, Richardson U, Nitsch RM, Wurtman RJ. Dioctanoylglycerol stimulates accumulation of [methyl- $^{14}\text{C}$ ]choline and its incorporation into acetylcholine and phosphatidylcholine in a human cholinergic neuroblastoma cell line. *Brain Res*. 1992;585:169–176.
19. Yorek MA, Dunlap JA, Spector AA, Ginsberg BH. Effect of ethanolamine on choline uptake and incorporation into phosphatidylcholine in human Y79 retinoblastoma cells. *J Lipid Res*. 1986;27:1205–1213.
20. Beheshti M, Imamovic L, Broinger G, et al.  $^{18}\text{F}$  choline PET/CT in the preoperative staging of prostate cancer in patients with intermediate or high risk of extracapsular disease: a prospective study of 130 patients. *Radiology*. 2010;254: 925–933.
21. Steuber T, Schlomm T, Heinzer H, et al. [ $^{18}\text{F}$ ]-fluoroethylcholine combined in-line PET-CT scan for detection of lymph-node metastasis in high risk prostate cancer patients prior to radical prostatectomy: Preliminary results from a prospective histology-based study. *Eur J Cancer*. 2010;46:449–455.
22. Piert M, Park H, Khan A, et al. Detection of aggressive primary prostate cancer with  $^{11}\text{C}$ -choline PET/CT using multimodality fusion techniques. *J Nucl Med*. 2009;50:1585–1593.
23. Yamamoto Y, Nishiyama Y, Kameyama R, et al. Detection of hepatocellular carcinoma using  $^{11}\text{C}$ -choline PET: comparison with  $^{18}\text{F}$ -FDG PET. *J Nucl Med*. 2008;49:1245–1248.
24. Talbot JN, Gutman F, Fartoux L, et al. PET/CT in patients with hepatocellular carcinoma using [ $^{18}\text{F}$ ]fluorocholine: preliminary comparison with [ $^{18}\text{F}$ ]FDG PET/CT. *Eur J Nucl Med Mol Imaging*. 2006;33:1285–1289.
25. Huang Z, Zuo C, Guan Y, et al. Misdiagnoses of  $^{11}\text{C}$ -choline combined with  $^{18}\text{F}$ -FDG PET imaging in brain tumours. *Nucl Med Commun*. 2008;29:354–358.
26. Kwee SA, Coel MN, Lim J, Ko JP. Combined use of F-18 fluorocholine positron emission tomography and magnetic resonance spectroscopy for brain tumor evaluation. *J Neuroimaging*. 2004;14:285–289.
27. Hara T, Kondo T, Hara T, Kosaka N. Use of  $^{18}\text{F}$ -choline and  $^{11}\text{C}$ -choline as contrast agents in positron emission tomography imaging-guided stereotactic biopsy sampling of gliomas. *J Neurosurg*. 2003;99:474–479.
28. Kwee SA, Ko JP, Jiang CS, Watters MR, Coel MN. Solitary brain lesions enhancing at MR imaging: evaluation with fluorine 18 fluorocholine PET. *Radiology*. 2007;244:557–565.
29. Tateishi U, Yamaguchi U, Maeda T, et al. Staging performance of carbon-11 choline positron emission tomography/computed tomography in patients with bone and soft tissue sarcoma: comparison with conventional imaging. *Cancer Sci*. 2006;97:1125–1128.
30. van den Brekel MWM, Runne RW, Smele LE, Tiwari RM, Snow GB, Castelijns JA. Assessment of tumour invasion into the mandible: the value of different imaging techniques. *Eur Radiol*. 1998;8:1552–1557.
31. Daisne JF, Duprez T, Weynand B, et al. Tumor volume in pharyngolaryngeal squamous cell carcinoma: comparison at CT, MR imaging, and FDG PET and validation with surgical specimen. *Radiology*. 2004;233:93–100.